Optical Engineering

SPIEDigitalLibrary.org/oe

Photonic crystal ring resonator-based add drop filters: a review

Savarimuthu Robinson
Rangaswamy Nakkeeran

SPIE

Optical Engineering 52(6), 060901 (June 2013)

REVIEW

Photonic crystal ring resonator-based add drop filters: a review

Savarimuthu Robinson
Mount Zion College of Engineering and Technology
Department of Electronics and Communication Engineering
Pudukkottai, Tamil Nadu 622 507, India
E-mail: mail2robinson@pec.edu

Rangaswamy Nakkeeran
Pondicherry Engineering College
Department of Electronics Engineering
Puducherry 605 014, India

Abstract. The add drop filter (ADF) is one of the most significant devices for coarse wavelength division multiplexing (CWDM) systems to add and/or drop a required channel individually from multiplexed output channels without disturbing other channels. The important parameters of the ADF are coupling efficiency, dropping efficiency, passband width and *Q* factor. Photonic crystal (PC)-based optical devices have attracted great interest due to their compactness, speed of operation, long life period, suitability for photonic integrated circuits, and future optical networks. Here, an extensive overview of a photonic crystal ring resonator (PCRR)-based ADF using a different shape of ring resonator is presented, and its corresponding functional parameters are discussed. Finally, the designed circular PCRR-based ADF for an ITU-T G 694.2 CWDM system is presented. Approximately 100% of coupling efficiency and dropping efficiency, 114.69 of *Q* factor, and 13 nm of passband width is obtained through simulation, which outperforms the reported one. [DOI: 10.1117/1.OE.52.6.060901]

Subject terms: photonic crystal; ring resonator; photonic band gap; add drop filter; photonic integrated circuits; two-dimensional; optical communication; coarse wavelength division multiplexing systems.

Paper 130083V received Jan. 18, 2013; revised manuscript received May 3, 2013; accepted for publication May 15, 2013; published online Jun. 12, 2013.

1 Introduction

The exponentially increasing bandwidth requirements for internet generation and multimedia applications is pushing optical communication ever closer to the (last mile) end user. The optical network system has penetrated into some local area networks through wavelength division multiplexing passive optical networks, metro and access networks from long-haul provision of data transportation. The more complex the network, the more nodes that are needed, each of which requires high functionality photonic integrated circuits (PIC). Developing ultra-small optical components for PICs is currently the subject of intense research. Generally, planar lightwave circuits (PLC), microelectromechanical systems (MEMS), and photonic crystals (PC) are providing a fascinating platform for a new generation of integrated optical devices and components of ultra-compact sizes[1] in the cm to μm range. PLC technology results in a device size in the cm to mm range and MEMS-based devices are developed between mm and μm. Even though MEMS-based devices are becoming smaller and smaller, they encounter radiation loss, lower life period (due to its movable components)[2] and high sensitivity when the size of the device is in the micrometre range. In contrast, PCs mitigate these issues without sacrificing performance.

Typically, the add drop filter (ADF) is one of the devices that receives prime consideration for use in coarse wavelength division multiplexing (CWDM) systems to add/drop a required wavelength channel without disturbing other channels arriving along with it. In an eight-channel ITU-T G. 694.2 CWDM system, the eight wavelengths (λ) are used to add/drop channels over the range from 1471 to 1611 nm with 20 nm channel spacing[3] and the passband width of the channel is 13 nm ($\pm$1.5 nm). Conventional ADFs, such as Bragg grating filters, Fabry–Perot filters, liquid crystal filters, acoustic optic filters, thin film filters, arrayed waveguide grating filters, and micro-ring resonator-based filters[4] are in the scale of centimetres, which may not be suitable for PICs. Among these various types of filters, the micro-ring resonator-based ADF is an attractive candidate for filtering purposes and contributing to a better response because of its circular resonating mode. However, when the radius of the ring resonator decreases below 5 μm, propagation and bending losses increase exponentially. They affect coupling and dropping efficiencies, passband width, and in turn, the *Q* factor of the filter. Photonic crystal ring resonator (PCRR)-based ADF is one of the right candidates to overcome this issue, as it does not allow these losses to increase exponentially.

Generally, PCs are composed of periodic dielectric or metallo-dielectric nanostructures that have alternating low and high dielectric constant materials (refractive index) in one, two, and three dimensions, which affect the propagation of electromagnetic waves inside the structure. As a result of this periodicity, PCs exhibit a unique optical property, namely, a photonic band gap (PBG) where electromagnetic mode propagation is absolutely zero due to reflection. PBG is the range of frequencies that neither absorbs light nor allows light propagation. By introducing a defect (point or line or both) in these structures, the periodicity and thus the completeness of the band gap are broken and the propagation of light can be localized in the PBG region.[5,6] Such an outcome allows realization of a wide variety of active and passive devices for optical communication. Compared with conventional optical devices, PC-based optical devices have attracted great interest due to their compactness (10 to

100 times) compared to conventional devices, high speed of operation, better confinement, suitability for integration, and the fact that device performance is not affected by miniaturization. PCs are basically classified into three types according to the orientation of their materials, namely, one-dimensional (1-D), two-dimensional (2-D) and three-dimensional (3-D) PCs. The first of these structures, originally proposed in 1887, is now known as 1-DPC. After a century, 2-DPC and 3-DPC were introduced. Out of these, 2-DPCs have refractive index changes in two perpendicular directions that play an important role in designing photonic devices due to ease in controlling their propagation modes, accurate calculation of PBG, efficient light confinement, simple design, and easy fabrication capability.[7]

In recent years, many PC-based optical devices have been proposed both theoretically and experimentally. To name a few, add-drop filters,[2] power splitters,[8–11] multiplexers and demultiplexers,[12–14] triplexers,[15] switches,[16] directional couplers,[17] bandstop filters,[18] bandpass filters,[19] and waveguides.[20]

In this paper, an overview of reported PCRR-based ADFs, such as square/quasi-square-shaped PCRR,[2,21,22] dual curved-shaped PCRR,[23] hexagonal-shaped PCRR,[24,25] 45-deg square-shaped PCRR,[26] diamond-shaped PCRR,[27] and X-shaped PCRR[28] are discussed in detail. To overcome the issues in the reported ADFs, a circular PCRR-based ADF is designed, and the coupling efficiency, dropping efficiency, Q factor and passband width are investigated. Then the filter parameters of the circular PCRR-based ADF are compared with the reported ones' parameters.

The rest of the paper is arranged as follows: In Sec. 2, the operating principle of the ring resonator-based ADF design is presented. An overview of reported PCRR-based ADFs is discussed in Sec. 3. The designed circular PCRR based ADF is described in Sec. 4, and Sec. 5 concludes the paper.

2 Optical Ring Resonator-Based ADF

An optical ring resonator is positioned between two optical waveguides to provide an ideal basic structure for a ring resonator-based ADF. In this structure, a bus waveguide can couple to the ring resonator at its resonant frequency to trap the electromagnetic energy that is propagating in the waveguide and localize it in the ring resonator. In other words, the light is dropped from the bus waveguide by the ring resonator and it is sent to the bottom waveguide. Figure 1 shows the schematic structure of the ring resonator-based ADF, which consists of the bus and dropping waveguides and the ring resonator (coupling element). Also, it has four ports; ports 1 and 2 are the input and transmission output terminals whereas ports 3 and 4 are forward and backward dropping terminals, respectively.

In PC structures, two kinds of optical resonators can be designed: (1) line defect or point defect-based resonators i.e., one where changing the size or dielectric constant of each rod causes the consequent defect to behave as a resonator. And (2) ring resonators i.e., if we remove some rods in order to have a ring shape, we have a ring resonator. For such devices, the choice of ring size is determined by the desired resonant wavelength and the tradeoff between the cavity Q and modal volume V.[2] Compared to point-defect or line-defect PC cavities, PCRRs offer scalability in size,

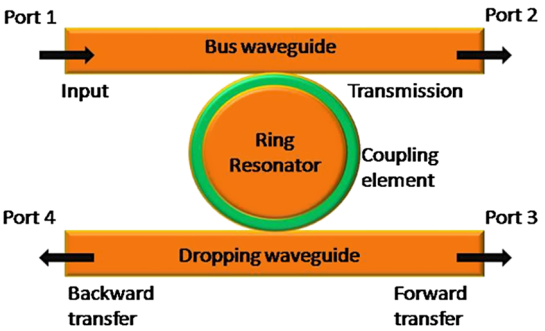

Fig. 1 Schematic structure of ring resonator based add drop filter (ADF).

flexibility in mode design due to their multimode nature,[29] and adaptability in structure design because of numerous design parameters. The design parameters can be the radius of the scatters, coupling rods, and the dielectric constant of the structure. Also, one of the advantages of PCRRs is their flexible design of backward and forward dropping. Owing to the above-mentioned reasons, here we have considered PCRR-based ADFs.

2.1 *Operating Principle*

If the ring resonator supports only one resonant mode, it will decay through both waveguides along the forward and backward directions, which introduces the reflection. Hence, in order for a complete transfer to happen, at least two modes are needed for the decaying amplitudes cancel either the backward direction or the forward direction of the bus waveguide.[29]

Two mirror planes can be considered for this structure, one perpendicular to the waveguides or one parallel to the waveguides. In order to cancel the reflected signal, a structure with a mirror plane symmetry perpendicular to both waveguides is considered. Assume that there exist two localized modes that have different symmetries with respect to the mirror plane: one has even symmetry and the other has odd symmetry. The even mode decays with the same phase into the forward and backward directions as shown in Fig. 2(a), however the odd mode decays into the forward direction out of phase with the decaying amplitude along the backward direction, as shown in Fig. 2(b). When the two tunneling processes come together, the decaying amplitudes into the backward direction of both waveguides are canceled, which is clearly depicted in Fig. 2(c). It should be noted that, in order for cancellation to occur, the line shapes of the two resonances should overlap. This means both resonances must have significantly the same resonant wavelength and the same bandwidth.

Also, due to the occurrence of degeneracy, the incoming wave interferes destructively with the decaying amplitude into the forward direction of the bus waveguides, causing all the power traveling in the bus waveguide to be cancelled. The symmetry of the resonant modes with respect to the mirror plane parallel to the waveguides determines the direction of the transfer wave in the ADF. For instance, as apparent from Fig. 2(a), 2(b), and 2(c), when both of the modes are even with regard to the parallel mirror plane, the decaying amplitudes along the backward direction of the drop waveguide would be canceled, allowing all the power to

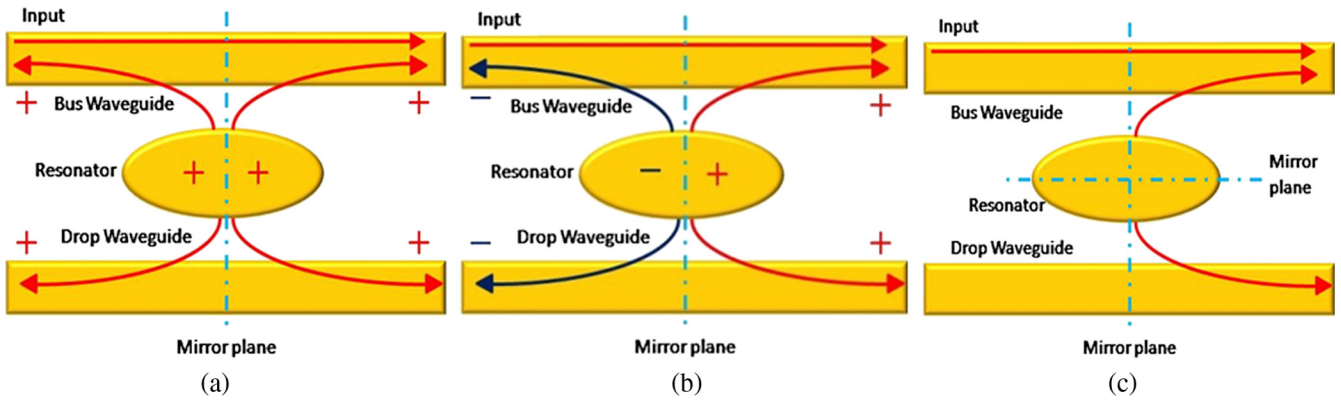

Fig. 2 Channel drop tunneling process for a resonator system that supports forward transfer of signal.

be transferred into the forward direction of the drop waveguide. On the other hand, the even mode could be odd with respect to the mirror plane parallel to the waveguides. When accidental degeneracy between the states occurs, the decaying amplitudes cancel in the forward direction of the drop waveguide [Fig. 3(a), 3(b), and 3(c)]. The entire power is transferred into the backward direction of the drop waveguide.[29]

PCRR resonant coupling occurs due to the frequency and phase matching between the propagating waveguide mode and the PCRR resonant cavity mode. The coupling direction is mainly determined by the modal symmetry and the relative coupling between the PCRRs. The direction is the same for the propagating wave in the waveguide and the coupled wave inside the PCRR. However, the direction may be the same or reverse for the coupling between PCRRs, depending upon coupling strength and modal symmetry.[29] Both forward dropping and backward dropping can be obtained depending upon the mode symmetry properties with respect to the coupling configurations.

2.2 *Requirements of the ADF*

The filter performance is determined by the transfer efficiency (coupling efficiency and dropping efficiency) between the two waveguides. Perfect efficiency corresponds to complete transfer of the selected channel in either the forward or backward direction in the dropping waveguide without forward transmission or backward reflection in the bus waveguide. All other channels remain unaffected by the presence of optical resonators.

To achieve complete transfer of the signal at resonance, the PCRR-based ADF must satisfy the following three conditions:

1. The resonator must possess at least two resonant modes, each of which must be even and odd with respect to the mirror plane of symmetry perpendicular to the waveguides.
2. The modes must degenerate.
3. The modes must have equal Q.

All three conditions are necessary to achieve complete transfer of the signal from the bus waveguide to the PCRR and for the PCRR to drop the waveguide.[30,31]

3 Photonic Crystal Ring Resonator-Based ADF: Types

In this section, the reported PCRR-based ADF is discussed. All the designs discussed in this section are based on 2-DPCs in square and triangular lattices. The reported PCRR-based ADFs are:

1. Square and quasi-square-shape PCRR,
2. Dual curved-shape PCRR,
3. Hexagonal-shape PCRR,
4. 45-deg-square shape PCRR,
5. Diamond-shape PCRR, and
6. X-shape PCRR.

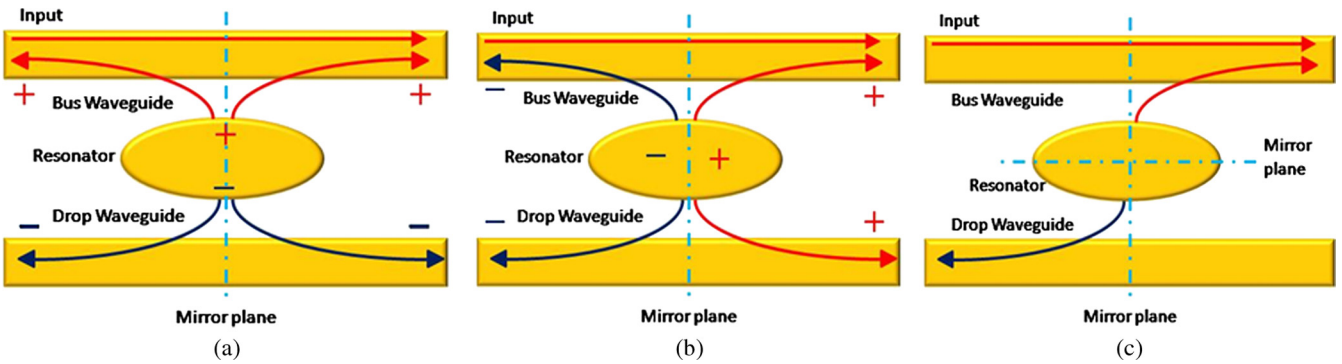

Fig. 3 Channel drop tunneling process for a resonator system that supports backward transfer of signal.

The coupling efficiency, dropping efficiency, Q factor, and passband width of the above mentioned PCRRs are discussed in the following section one by one.

3.1 *Square/Quasi-square-Shape Photonic Crystal Ring Resonator*

The structure[21] under consideration is a 2-D pillar type PC and consists of an array of rods in a square lattice, as shown in Fig. 4. The refractive index of the dielectric rods is 3.59, surrounded by the background of air ($n = 1.00$). The radius of the rod and the lattice constant (distance between two adjacent rods) is 100 and 540 nm, respectively. The transverse magnetic (TM) band gap range of the structure is $0.303a/\lambda$ to $0.425a/\lambda$, whose corresponding wavelength range spans from 1270 to 1740 nm where "a" is the lattice constant and "λ" is the free space wavelength.

The square PCRR-based ADF (Fig. 4) consists of two waveguides in the horizontal ($\Gamma - x$) direction and a square-shaped PCRR positioned between them. The top waveguide is called a bus waveguide whereas the bottom waveguide is known as the dropping waveguide. The input signal port is marked "A" with an arrow on the left side of bus waveguide. The ports "C" and "D" of the drop waveguide is the drop terminals and denoted as forward dropping and backward dropping, respectively, while port "B" on the right side of bus waveguide is designated as forward transmission terminal.

Fig. 4 Schematic structure of square shape photonic crystal ring resonator (PCRR) based ADF.

The bus and the dropping waveguides are formed by introducing line defects whereas the square PCRR is shaped by creating point defects (i.e., by removing the columns of rods to make a square shape). The rods located inside the square PCRR are called inner rods whereas the coupling rods are those placed between the square PCRR and the waveguides. At resonance, the wavelength is coupled from the bus waveguide into the dropping waveguide and exits through one of the output ports. The coupling and dropping efficiencies are detected by monitoring the power at ports "B" and, "C" and "D", respectively. The normalized transmission spectra of square PCRR-based ADF is depicted in Fig. 5(b) (red color) where the coupling efficiency, dropping efficiency, and spectral selectivity of the filter is also poor.

In order to improve the coupling efficiency, dropping efficiency, and spectral selectivity by suppressing the counter-propagation modes, the rods with blue color, so-called scatterer rods (labeled "s") are placed at each corner of the four sides with a half-lattice constant that turns the square structure into a quasi-square structure. Consequently, the counter propagation modes can cause spurious dips in the transmission spectrum.

The schematic structure and the normalized transmission spectra of quasi-square PCRR-based ADF are shown in Fig. 5(a) and 5(b), respectively. A Gaussian optical pulse, covering the whole frequency-range-of-interest, is launched at the input port A. Power monitors were placed at each of the other three ports (B, C, D) to collect the transmitted spectral power density after Fourier transformation. All of the transmitted spectral power densities were normalized to the incident light spectral power density from input port "A".

The resonant wavelength, coupling efficiency, dropping efficiency, and Q factor of the quasi-square PCRR-based ADF are 1567 nm, 100%, 98%, and 160, respectively. It is noted that, for a cavity without scatterer rods, low coupling (90%) and dropping efficiency (75%) with poor spectral selectivity is obtained. By simply introducing four scatterers, the performance of the ADF is greatly improved. The Q factor (spectral selectivity) can be improved by increasing coupling rods between the ring resonator and the waveguide. However, there is a trade-off between the increase of the cavity Q and decrease the coupling and dropping efficiency.

The quasi-square PCRR-based ADF is further designed to improve the passband width. The passband width can

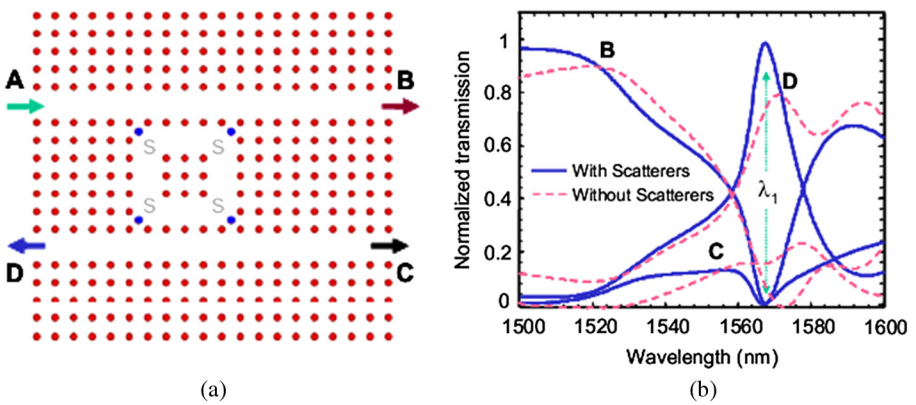

(a) (b)

Fig. 5 (a) Schematic structure and (b) normalized transmission spectra of quasi-square PCRR based ADF.

be increased by improving the coupling between the waveguide and resonator, which could be done by reducing the coupling rod's radius. In this structure,[22] the size of the coupling rods is 99 nm.

Figure 6(a) and 6(b) depicts the schematic structure and its normalized transmission spectra of the quasi-square PCRR-based ADF with a coupling rod radius of 99 nm. The resonant wavelength of the structure is 1567 nm. As seen in Fig. 6(b), the transmission in the drop waveguide is about 98% at resonance, and the transmitted flux in the bus waveguide is about 96%. The passband width and Q factor of this structure is 30 nm and 52.33, respectively.

3.2 *Dual-Curved Photonic Crystal Ring Resonator*

This ADF consists of a dual curved PCRR[23] that is placed between two open-ended waveguides, which is demonstrated in Fig. 7(a). The resonator is two coupled curved Fabry–Perot resonators, each or which is a Fabry–Perot cavity with a curved structure rather than a straight closed waveguide. The length and curvature radius of resonator could be selected according to conditions for having more compact photonic crystal optical integrated circuits, a specific operational wavelength, enlarging mode spacing or higher quality factor and drop efficiency.

The structure consists of a background of BSC glass and the rods GaAs having a refractive index of 1.507 and 3.57, respectively. The radius of the rod (r) is $0.2a$ where a is 487 nm. The normalized frequency range is $0.259a/\lambda$ to $0.325a/\lambda$. The dual curved PCRR consists of two curved Fabry–Perot resonators, in which energy can be exchanged between them by means of evanescent wave coupling.[23] In the resonator, facing two curved cavities toward each other causes three contact points with high coupling intensity instead of the single one found in coupled ordinary Fabry–Perot or ring resonators. The Q factor, reflected power to the input port, drop efficiency, and transmission spectra are affected by the barrier thickness between two coupled resonators. Therefore these variations can be investigated by altering the number of spacer rods. Results show that the best dropping occurs with a two-rod spacer between two coupled resonators. This result has been expected since Fabry–Perot cavities have larger overlap with the other defects in the angle of 60-deg with respect to their axes.

The resonator resonates at $\lambda = 1551.3$ nm; the Q factor of this resonator is 153.6 and its drop efficiency is 68%. The Q factor of this ADF increases by enhancing the period of the coupling section between the resonator and two open-ended waveguides, however drop efficiency decreases.

3.3 *Hexagonal-Shaped Photonic Crystal Ring Resonator*

The hexagonal PCRR-based ADF[24] is designed by 2-DPC in a triangular lattice. The radius of the rod is $0.2a$ where a is a lattice constant i.e., 410 nm. The normalized frequency of

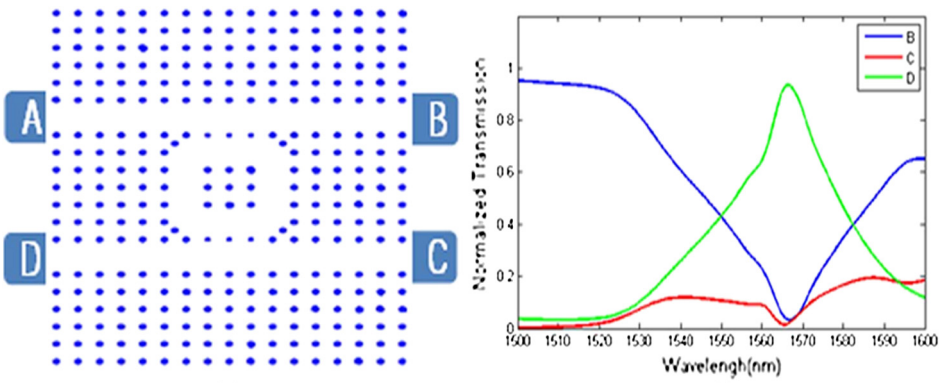

Fig. 6 (a) Schematic structure and (b) normalized transmission spectra of quasi-square PCRR based ADF.

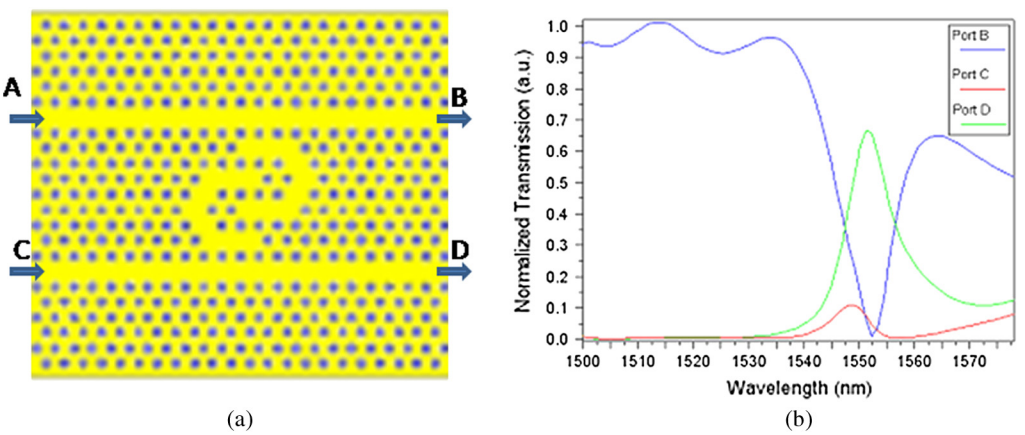

Fig. 7 (a) Schematic structure and (b) normalized transmission spectra of dual curved PCRR based ADF.

TM PBG is $0.252a/\lambda$ to $0.314a/\lambda$ and its corresponding wavelength range spans from 1305 to 1626 nm. The circular rod is embedded in the air host. The line and point defects are introduced to make the hexagonal shape between the waveguides.

The schematic structure and normalized transmission spectra of the hexagonal PCRR-based ADF is shown in Fig. 8(a) and 8(b), respectively. A resonant peak reveals at 1564.5 nm with a quality factor of 423. The coupling and dropping efficiency noticed from the spectra are 98% and 60%, respectively.

Earlier, a hexagonal PCRR-based ADF was presented where the inner and outer shape of the cavity was hexagonal [as can be seen in Fig. 8(a)]. Here, a hexagonal PCRR-based ADF with circular rods is described. The inner rods are shifted toward to centre to make a circular shape inside the cavity. The structural parameters (lattice constant, radius of the rods, refractive index of the rods, and background index) employed in this design are similar to those in the previous design. The schematic structure and normalized transmission spectra of the modified hexagonal PCRR-based ADF is shown in Fig. 9(a) and 9(b), respectively. The resonant wavelength, coupling efficiency, dropping efficiency and Q factor of the modified hexagonal PCRR based-ADF[25] is 1553 nm, 90%, 70%, and 108, respectively.

To achieve high dropping efficiency with the optimized hexagonal PCRR, two scatterer rods, the same as other rods labeled "s", are incorporated. The schematic structure and normalized transmission spectra of the modified hexagonal PCRR-based ADF with scatterer rods are shown in Fig. 10(a) and 10(b), respectively. The introducing of these scatterers improves spectral selectivity by enhancing the dropping efficiency to about 95% at the resonant wavelength of 1550 nm while the quality factor is also increased to 245.

3.4 *45-deg Square-Shaped Photonic Crystal Ring Resonator*

The schematic diagram of a 45-deg PCRR-based ADF[26] is shown in Fig. 11(a), and is a square lattice with silicon rods in air. The Si rod with a refractive index of 3.48 is embedded in the air. The radius of the rod is $0.1a$ where "a" is 685 nm. The TM PBG range of this structure is $0.395a/\lambda$ to $0.505a/\lambda$. The line and point defects are introduced in the angle of 45 deg to devise the PCRR, and two scatterer rods are introduced in each ending point of the corner to enhance the spectral selectivity and in turn, coupling and dropping efficiency.

The normalized spectra of the 45-deg PCRR-based ADF is shown in Fig. 11(b). The resonant wavelength, dropping efficiency, and Q factor is 1550 nm, 90%, and 840, respectively. The discrepancy between the ideal PCRR Q and the ADF Q is mainly caused by the coupling strength and the coupling sections between the waveguide and PCRR ring.

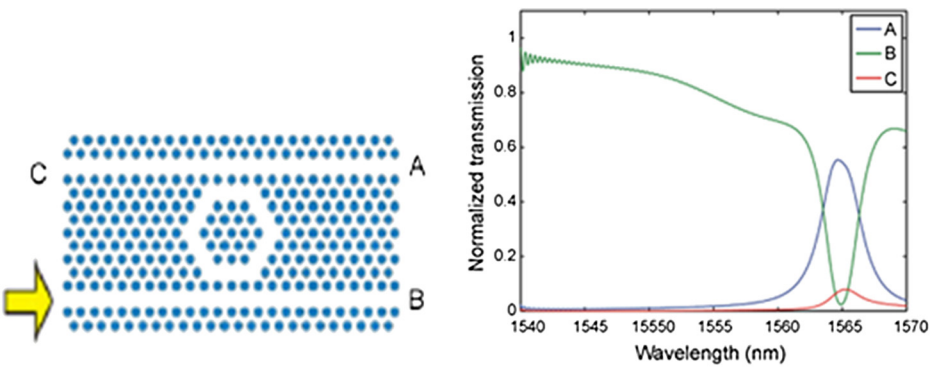

Fig. 8 (a) Schematic structure and (b) normalized transmission spectra of hexagonal PCRR based ADF.

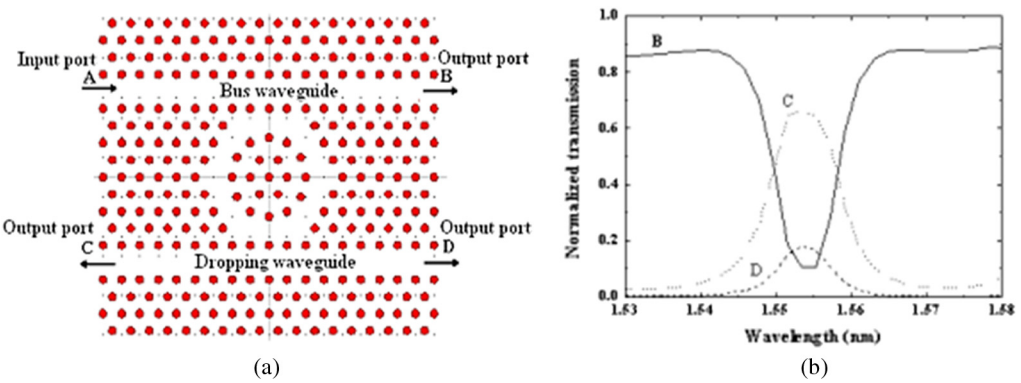

Fig. 9 (a) Schematic structure and (b) normalized transmission spectra of quasi-square PCRR based ADF.

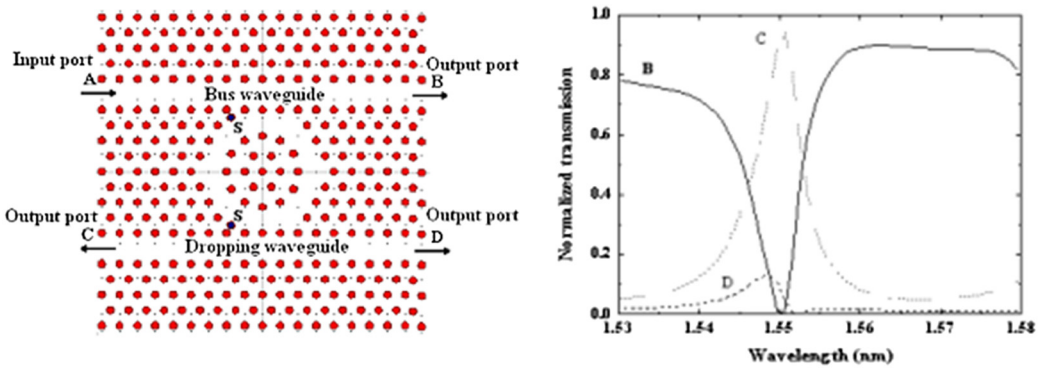

(a) (b)

Fig. 10 (a) Schematic structure and (b) normalized transmission spectra of quasi-square PCRR based ADF.

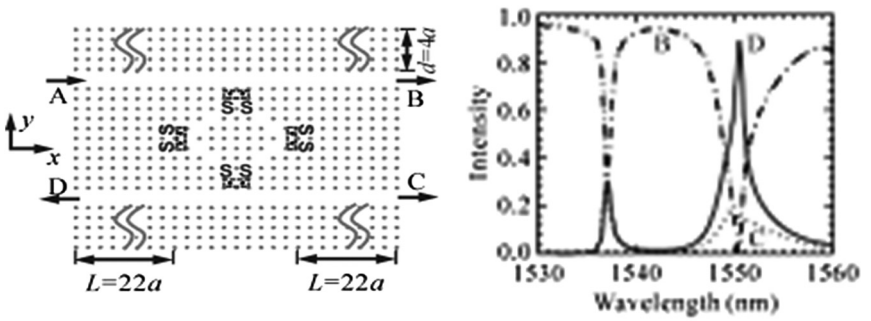

(a) (b)

Fig. 11 (a) Schematic structure and (b) normalized transmission spectra of quasi-square PCRR based ADF.

3.5 *Diamond-Shaped Photonic Crystal Ring Resonator*

The triangular lattice of air holes in the dielectric and the dielectric is assumed to be chalcogenide glass, which has a linear refractive index of $n = 3.1$ and the radius of the air holes $r = 0.32a$.[27] The PC waveguides are created like defects by setting the radius of the line air holes as $r = 0.12a$. PC waveguides are created as line defects by setting the radius of line air holes to be $rd = 0.12a$ instead of removing them perfectly. The modal patterns in such a structure can spread more into the defect near the waveguide and hence the tunneling effect can be strengthened. The angle of the line defects that are introduced to create a diamond shape is 120 deg. The schematic structure and normalized transmission spectra of the diamond PCRR-based ADF is shown in Fig. 12(a) and 12(b), respectively.

The TM PBG range of the structure is between $0.248a/\lambda$ and $0.272a/\lambda$. The resonant frequency of the ADF is $0.2518a/\lambda$. The dropping efficiency of the diamond-shaped PCRR is 75%. The dropping efficiency is greatly affected by the length of the Fabry–Perot resonators.

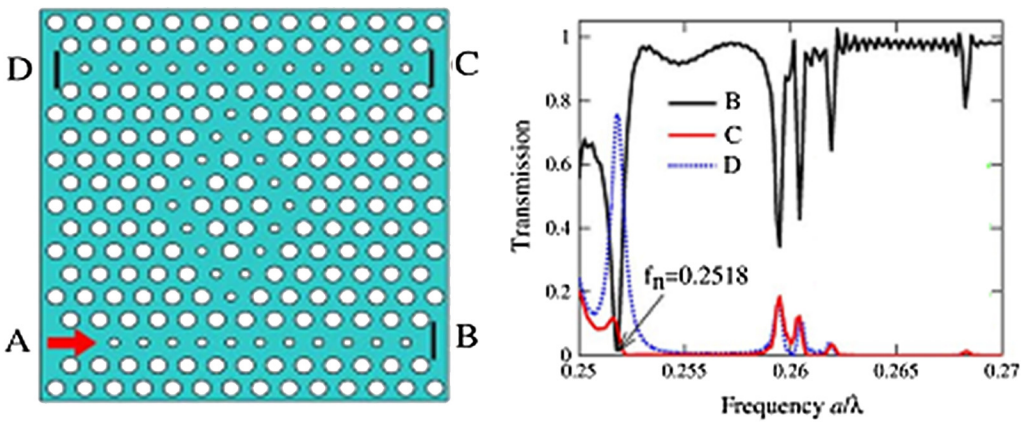

(a) (b)

Fig. 12 (a) Schematic structure and (b) normalized transmission spectra of diamond PCRR based ADF.

3.6 *X-Shaped Photonic Crystal Ring Resonator*

The design of the X-shaped PCRR-based ADF[28] is based on a 2-D triangular lattice of silicon rods. The refractive index of an Si rod is 3.46, and they are embedded in an air background ($n_{air} = 1.00$). The schematic structure and normalized transmission spectra of the X-shaped PCRR-based ADF is shown in Fig. 13(a) and 13(b), respectively. The ratio of the rod radius r to the lattice constant a is 0.2.

The structure has a PBG only for the TM polarization with a single-mode frequency (normalized) ranging from $0.337a/\lambda$ to $0.442a/\lambda$, where the lattice constant a is set at 607.6 nm. Eight additional scatterer rods are incorporated to improve the spectral selectivity and obtain a very high dropped efficiency.[10] These scatterers have exactly the same refractive indices as all other dielectric rods in the PC structure and their diameters are chosen to be $r = 0.965r$ for better performance. It is clear from Fig. 13(b) that close to 100% (>99.98%) dropping efficiency is noticed at the resonant frequency of 1550 nm. The Q factor of the forward dropping peak is 196.

It is very clear that a single PCRR is responsible for single resonant wavelength. Hence, it is also possible to get two or more resonant wavelengths by cascading the single PCRR. The dual PCRR-based ADF is also investigated for quasi-square PCRR[2] and 45-deg PCRR.[26] The performance of these filters is not better than that of the micro ring resonators.

To summarize, the important ADF parameters, i.e., coupling efficiency, dropping efficiency, resonant wavelength, passband width, and Q factor of the reported PCRR-based ADF, is highlighted. In the above discussion, PCRR-based ADFs are designed by pillar type (rod) or membrane type (hole) in either a square lattice or a triangular lattice, and structural parameters such as radius of the rod, lattice constant, and refractive index are chosen according to their requirements. Out of eight PCRR-based ADF, the quasi-square PCRR-based ADF[2] and X-shaped PCRR-based ADF23 provides better performance than the others, however, it has not reached 100% of dropping efficiency. This is due to the proper corners in the PCRRs. In the aforementioned PCRR-based ADFs, the PCRR has a proper corner that reduces the output power at resonance owing to scattering at corners. To overcome the above issue, the author proposed[32] and designed a circular PCRR-based ADF where the circular ring resonator has gradual changes at corners. As this is subtle in nature, it reduces scattering and improves the output efficiency through circular resonant modes. The ring resonator-based ADF also provides efficient wavelength selection, scalability, narrow linewidth, flexibility in mode design, and smaller channel spacing. Even though the triangular lattice offers wider bandgaps than the square lattice, the square lattice PC-based ADF provides effective confinement of light, easy fabrication, simple structure, and easily controllable propagation modes. Typically, pillar-based PCs have several advantages such as low out-of-plane losses, propagation loss, easy fabrication, compatibility with classical PICs, and effective single mode operation due to defects-based structure.[33] Owing to the above mentioned advantages, we conceived a 2-D pillar-type circular PCRR-based ADF design in a square lattice. The details of the circular PCRR-based ADF are discussed in the next section.

4 Circular Photonic Crystal Ring Resonator

The circular PCRR-based ADF is designed using 2-D PCs with circular rods in the square lattice. The number of rods in the X and Z directions is 21. The distance between the two adjacent rods is 540 nm, which is termed as lattice constant a. The Si rod with a refractive index of 3.47 is embedded in the air. The radius of the rods is 0.1 μm and the overall size of the device comes to around 11.4×11.4 μm. The optimized values to design the ADF are obtained through the gap map, which gives the variation in TE/TM PBG with respect to the change of structural parameters.

Figure 14(a) shows the schematic structure of the circular PCRR-based ADF. The details and its operation are explained later part of this section. The band diagram in Fig. 14(b) gives the propagation modes and PBG of the PC structure, which has TM PBG ranging from $0.295a/\lambda$ to $0.435a/\lambda$, and whose corresponding wavelength lies between 1241 and 1830 nm. It covers the entire wavelength range of third optical communication window. The guided

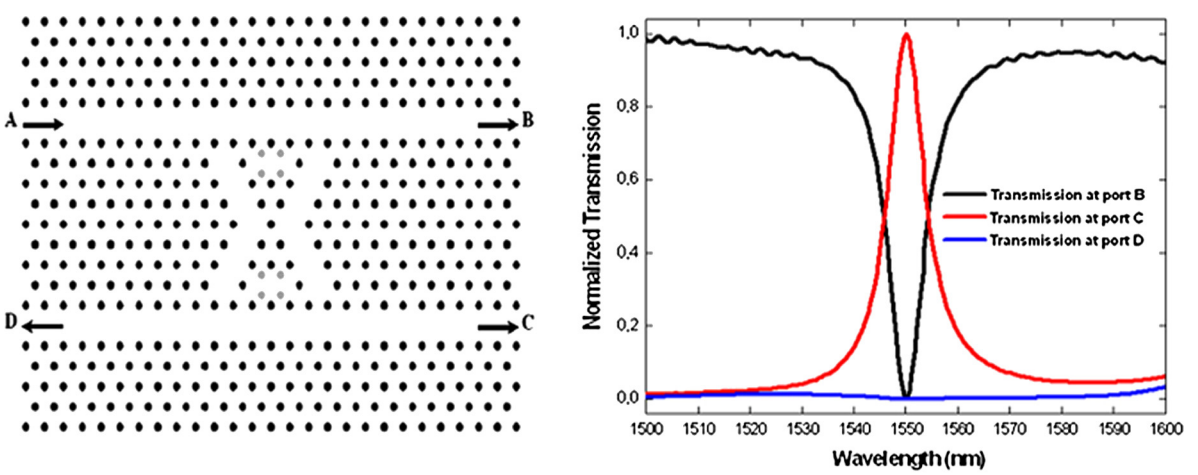

(a) (b)

Fig. 13 (a) Schematic structure and (b) normalized transmission spectra of X-shaped PCRR based ADF.

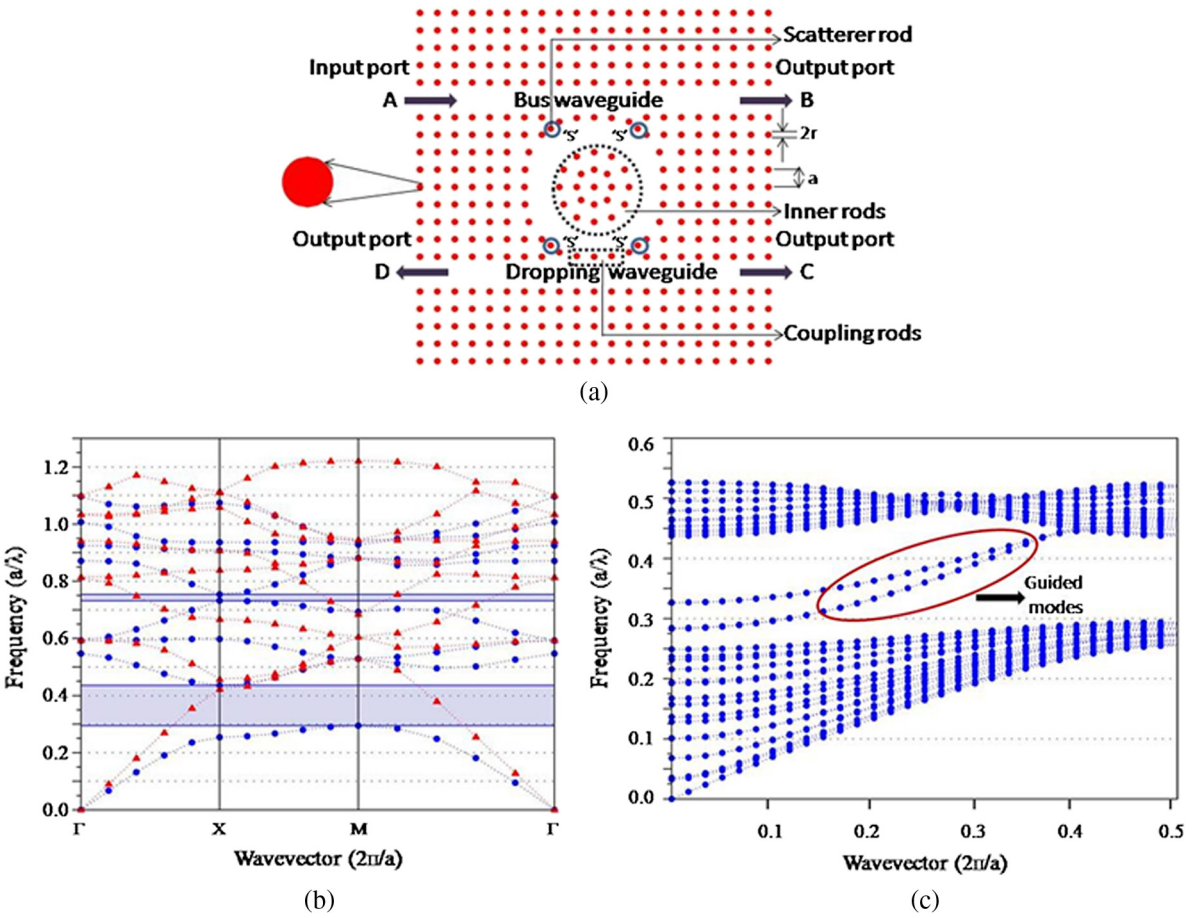

Fig. 14 (a) Schematic structure of circular PCRR based ADF, (b) band diagram of 1×1 PC (unit cell), and (c) band diagram of 21×21 PC (super cell) structure after the introduction of line and point defects.

modes (even and odd) inside the PBG region resulting from line and point defects (21×21 PC), shown in Fig. 14(c), supports the complete channel transfer and, in turn, higher output efficiency at resonance. The structure is surrounded by perfect matched layers as absorbing boundary conditions to truncate the computational regions and to avoid reflections from the boundary.[34]

The normalized transmission spectra of the circular PCRR-based ADF is obtained using the 2-D Finite Difference Time Domain (FDTD) method. Although the real SOI structure, would, in practice, require 3-D analysis, the 2-D approach gives a general indication of the expected 3-D behavior. 2-D analysis carried out here allows us to identify qualitatively many of the issues in the cavity design (e.g., mode control, cavity Q and the placement of the scatterers in the quasi-square ring cavity) and the coupling scheme design. This can reveal the design's trade-offs and guidelines before the real structure design based on a completely 3-D FDTD technique, which is typically computationally time and memory consuming.

The circular PCRR is constructed by varying the position of both inner rods and outer rods from their original position toward the centre of the origin (Γ). The inner rods are built by varying the position of adjacent rods on the four sides, from their centre, by 25%; on the other hand, the outer rods are constructed by varying the position of the second rod on the four sides, from their centre, by 25% in both X and Z directions. The number of rings that are formed by the ring is three. In order to improve the coupling efficiency, dropping efficiency, and spectral selectivity by suppressing the counter propagation modes, the scatterer rods (s) are placed at each corner of the four sides with a half lattice constant. The material properties and dimension of the scatterer rods are similar to the other rods. At resonance, the wavelength is coupled from the bus waveguide into the dropping waveguide and exits through one of the output ports. The coupling and dropping efficiencies are detected by monitoring the power at ports B, C, and D, respectively.

4.1 *Simulation Results and Discussions*

A Gaussian input signal is launched into the input port. The normalized transmission spectra at ports B, C, and D are obtained by conducting a fast Fourier transform of the fields that are calculated by the 2-D-FDTD method. The input and output signal power is recorded through power monitors by placing them at appropriate ports. The normalized transmission is calculated through the following formula:

$$T(f) = \frac{1/2 \int \text{real}(p(f)^{\text{monitor}}) \cdot \text{d}S}{\text{Source Power}},$$

where $T(f)$ is normalized transmission which is a function of frequency, $p(f)$ is poynting vector, and dS is the surface normal. The normalization at the output side does not affect the result because of source power normalization. Finally, the $T(f)$ is converted as a function of wavelength.

Figure 15 shows the normalized transmission spectra of circular PCRR-based ADF. The resonant wavelength of the ADF is observed at 1491 nm. The simulation shows 100% coupling and dropping efficiencies and its passband width is 13 nm. The Q factor, which is calculated as $\lambda/\Delta\lambda$ (resonant wavelength/full width half maximum), equals almost 114.69. The obtained results meet the requirements of ITU-T G 694.2 CWDM systems. The inset in Fig. 15 depicts the electric field pattern of pass and stop regions at 1491 and 1515 nm, respectively. At a resonant wavelength, $\lambda = 1491$ nm, the electric field of the bus waveguide is fully coupled with the ring and reached into its output port D. In this condition there is no signal flow in port B. Similarly, at off resonance, $\lambda = 1515$ nm, the signal directly reaches the transmission terminal (the signal is not coupled into the ring). The filter parameters of the newly designed filter are compared with the existing PCRR-based ADFs available in the literature are listed in Table 1.

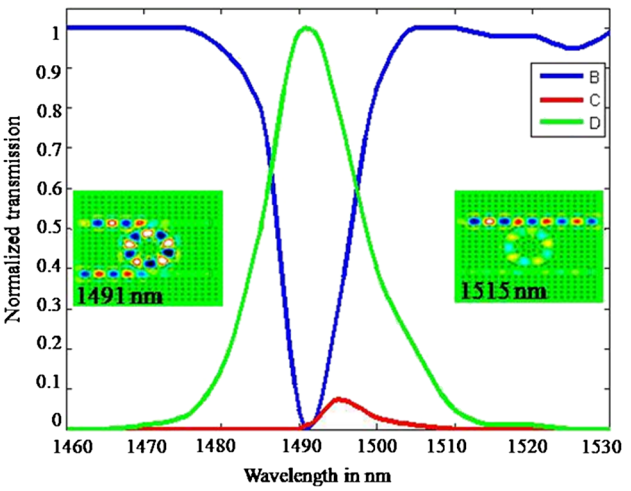

Fig. 15 Normalized transmission spectra of circular PCRR based ADF.

5 Conclusions

The CWDM system has recently emerged as a cost-effective solution for networks (metro/access, enterprise, and regional) requiring fairly high bit rates (1 to 40 Gbps), at minimal cost with unamplified point-to-point transport of several wavelengths over moderate distances (0 to 500 km). The ADF is one such device, and it receives prime consideration for CWDM networks to add/drop a required wavelength channel without disturbing other channels arriving along with them. A detailed survey of reported PCRR-based ADFs is presented, which has some limitations. To overcome these, the circular PCRR-based ADF is designed using circular rods to add/drop a channel at a centre wavelength of 1491 nm. Approximately 100% of coupling and dropping efficiencies are observed at 1491 nm. The passband width and Q factor of the designed ADF is 13 nm and 114.69, respectively. The suggested ADF is compact and the overall size of the chip is around 11.4×11.4 μm. Therefore, this kind of device would be more useful for the realization of integrated optic circuits for CWDM systems and, future access and metro networking applications.

Table 1 Comparison of proposed circular PCRR based ADF with the reported PCRR based ADF.

Parameters/Authors	CE(%)	DE(%)	Q factor	PW (nm)	Cavity Type
Qiang et al. (2007)	100	96	160	9.80	Quasi-square PCRR
Djavid et al. (2008)	99	99	52.73	30	Quasi-square PCRR
Andalib et al. (2008)	98	68	153.60	9.80	Dual curved PCRR
Monifi et al. (2009)	97	98	62.72	25	Quasi-square PCRR
Hsiano et al. (2009)	97	55	423	3.69	Hexagonal PCRR
Zheng et al. (2009)	100	95	245	6.32	Hexagonal PCRR
Mai et al. (2011)	98	58	313	5	Hexagonal PCRR
Bai et al, (2010)	100	90	840	1.85	45-deg PCRR
Ma et al. (2011)	100	95	775	2	Diamond shape PCRR
Mohmoud et al. (2012)	100	99.98	196	7.90	X-shaped PCRR
This work	100	100	114.60	13	Circular PCRR

NOTE: CE → Coupling Efficiency, DE → Dropping Efficiency; PW → Passband Width.

References

1. T.-T. Shih, Y.-D. Wu, and J.-J. Lee, "Proposal for compact optical triplexer filter using 2-D Photonic crystals," *IEEE Photon. Technol. Lett.* **21**, 18–21 (2009).
2. Z. Qiang, W. Zhou, and R. A. Soref, "Optical add-drop filters based on photonic crystal ring resonators," *Opt. Express* **15**(4), 1823–1831 (2007).
3. ITU Telecommunication Standardization Sector, "Spectral grids for WDM applications: CWDM wavelength grid," ITU-T Recommendation G 694.2 (2003).
4. D. Sadot and E. Boimvich, "Tunable optical filters for dense WDM networks," *IEEE Commun. Mag.* **36**(12), 50–55 (1998).
5. E. Yablonovitch, "Inhibited spontaneous emission on solid-state physics and electronics," *Phys. Rev. Lett.* **58**(20), 2059–2062 (1987).
6. S. John, "Strong localization of photons in certain disordered dielectric superlattices," *Phys. Rev. Lett.* **58**(23), 2486–2489 (1987).
7. J. D. Joannopoulos et al., *Photonic Crystal: Modeling of Flow of Light*, Princeton University Press, Princeton, New Jersey (2008).
8. A. Ghaffari et al., "Analysis of photonic crystal power splitters with different configurations," *J. Appl. Sci.* **8**(8), 1416–1425 (2008).
9. S. Huang et al., "Power splitters with different output power levels built with two dimensional photonic crystals," *Opt. Eng.* **45**(2), 020502 (2006).
10. Z. Wu et al., "Bends and splitters for self-collimated beams in two dimensional triangular lattice photonic crystals," *Opt. Eng.* **50**(11), 1140021 (2011).
11. T. Yu et al., "Power splitter based on photonic crystal waveguides with an air holes array," *Opt. Eng.* **50**(11), 1146011 (2011).
12. G. Manzacca et al., "2D photonic crystal cavity-based WDM multiplexer," *Photon. Nanostruct.* **5**(4), 164–170 (2007).
13. A. Ghaffari et al., "Heterostructure wavelength division demultiplexers using photonic crystal ring resonators," *Opt. Commun.* **281**(15–16), 4028–4032 (2008).
14. H. Ren et al., "Design of reconfigurable optical add/drop multiplexer based on two dimensional photonic crystals," *Opt. Eng.* **47**(12), 123001 (2008).
15. D. S. Park et al., "Photonic crystal-based GE-PON triplexer using point defects," *Proc. SPIE* **6897**, 689711 (2008).
16. Q. Wang et al., "The position independence of heterostructure coupled waveguides in photonic-crystal switch," *Optik (Munich, Ger.)* **121**(8), 684–688 (2010).
17. M. K. Moghaddam, A. R. Attari, and M. M. Mirsalehi, "Improved photonic crystal directional coupler with short length," *Photon. Nanostruct.* **8**(1), 47–53 (2010).
18. F. Monifi et al., "A new bandstop filter based on photonic crystals," in *Proc. Progress in Electromagnetic Research*, Cambridge, pp. 674–677 (2008).
19. C. Chao et al., "Bandpass filters based on phase-shifted photonic crystal waveguide gratings," *Opt. Express* **15**(18), 11278–11284 (2007).
20. N. Janrao, R. Zafar, and V. Janyani, "Improved design of photonic crystal waveguides with elliptical holes for enhanced slow light performance," *Opt. Eng.* **51**(6), 064001 (2012).
21. M. Djavid and M. S. Abrishanian, "Photonic crystal channel drop filters with mirror cavities," *Opt. Quantum Electron.* **39**(14), 1183–1190 (2007).
22. F. Monifi et al., "Three output port channel drop filter based on photonic crystals," *Appl. Opt.* **48**(4), 804–809 (2009).
23. P. Andalib and N. Granpayeh, "Optical add/drop filter based on dual curved photonic crystal resonator," in *IEEE Conf. on Photonics*, Freiburg, Germany, pp. 249–250 (2008).
24. F.-L. Hsiao and C. Lee, "A nano ring resonator based on 2D hexagonal lattice photonic crystals," in *IEEE Conf. on Optical MEMS and Nanophotonics*, Clearwater, Florida, pp. 107–108 (2009).
25. Y. Zheng, S. Li, and J. Kang, "Two dimensional photonic crystal channel filter based on ring resonator," in *IEEE Conf. on Photonics and Optoelectronics*, Wahun, China, pp. 1–3 (2009).
26. B. Jibo et al., "Characteristics of 45° photonic crystal ring resonators based on square lattice silicon rods," *Optoelectron. Lett.* **6**(3), 203–206 (2010).
27. Z. Ma and K. Ogusu, "Channel drop filters using photonic crystal Fabry–Perot resonators," *Opt. Commun.* **284**(5), 1192–1196 (2011).
28. M. Youcef et al., "Optical channel drop filters based on photonic crystal ring resonators," *Opt. Commun.* **285**(3), 368–372 (2012).
29. C. Manolatou et al., "Coupling of modes analysis of resonant channel add-drop filters," *IEEE J. Quantum Electron.* **35**(9), 1322–1331 (1999).
30. S. Fan et al., "Channel drop filters in photonic crystals," *Opt. Express* **3**(1), 4–11 (1998).
31. T. Baba, "Slow light in photonic crystals," *Nature* **2**(8), 465–473 (2008).
32. S. Robinson and R. Nakkeeran, "Coupled mode theory analysis for circular photonic crystal ring resonator based add drop filter," *Opt. Eng.* **51**(11), 114001–114006 (2012).
33. A. A. M. Kok et al., "Reduction of propagation loss in pillar-based photonic crystal waveguides," *J. Lightwave Technol.* **27**(17), 3904–3911 (2009).
34. A. Lavrinenko et al., "Comprehensive FDTD modeling of photonic crystal waveguide components," *Opt. Express* **12**(2), 234–248 (2004).

Savarimuthu Robinson received BE degree in electronics and communication engineering from Bharathidasan University, Tamil Nadu, India and ME degree in optical communication from Alagappa Chettiar College of Engineering and Technology, Karaikudi, Tamil Nadu, India, in 2004 and 2008, respectively. He is currently working toward the PhD degree at the Department of Electronics and Communication Engineering, Pondicherry Engineering College, Puducherry, India. He is currently working as an associate professor in the Department of Electronics and Communication Engineering, Mount Zion College of Engineering and Technology, Pudukkottai, Tamil Nadu. He is a life member of ISTE and IEEE. His current research interests are in the areas of optical communication, photonic crystals, photonic integrated circuits and optical networks.

Rangaswamy Nakkeeran received BSc degree in science and BE degree in electronics and communication engineering from Madras University in 1987 and 1991, respectively and ME degree in electronics and communication engineering (with diversification in optical communication) from Anna University in 1995. He received PhD degree from Pondicherry University in 2004. Since 1991, he has been working in the teaching profession. Presently, he is associate professor in Pondicherry University. He is life member of IETE, ISTE, OSI, and IE(I). Also, he is member of OSA, SPIE, IEICE, and IEEE. He has published more than 150 papers in National and International Conference Proceedings and Journals. He has coauthored a book published by PHI. His areas of interest are optical communication, networks, antennas, electromagnetic fields and wireless communication.